Soft Matter

ARTICLE TYPE

Cite this: DOI: 00.0000/xxxxxxxxxx

Effect of the interaction strength and anisotropy on the diffusio-phoresis of spherical colloids – Online Supplementary Material

Jiachen Wei,[a,b] Simón Ramírez-Hinestrosa,[b] Jure Dobnikar, [b,c,d]* and Daan Frenkel[b]†

Received Date
Accepted Date

DOI: 00.0000/xxxxxxxxxx

Gradients in temperature, concentration or electrostatic potential cannot exert forces on a bulk fluid; they can, however, exert forces on a fluid in a microscopic boundary layer surrounding a (nano)colloidal solute, resulting in so-called phoretic flow. Here we present a simulation study of phoretic flow around a spherical colloid held fixed in a concentration gradient. We show that the resulting flow velocity depends non-monotonically on the strength of the colloid-fluid interaction. The reason for this non-monotonic dependence is that solute particles are effectively trapped in a shell around the colloid and cannot contribute to diffusio-phoresis. We also observe that the flow depends sensitively on the anisotropy of solute-colloid interaction.

1 Size effect

The dependence of fluid velocity v_x on solute-colloid interaction strength in a bigger box of $N = 7700$ particles is shown in Fig. 1 below. For colloid with isotropic interaction, the increase of box size slightly reduces the magnitude of fluid velocity. However, for colloid with anisotropic interaction, the value of v_x is barely changed with the increase of N. This is because the asymmetric distribution of excess solute is observed even for $r > r_{cut}$ for system with isotropic interaction, but for system with anisotropic interaction the asymmetric distribution is observed locally within the cut-off.

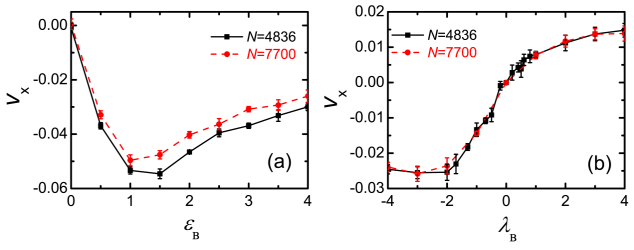

Fig. 1 The dependence of fluid velocity v_x on (a) isotropic ε_B and (b) anisotropic λ_B solute-colloid interaction strength, in simulation box containing $N = 4836$ or $N = 7700$ particles.

To further analyze the size effect on phoresis for system with isotropic interactions, in Fig. 2 we present the dependence of v_x on N at $\varepsilon_B = 1.5$ for slip and non-slip boundaries. We find the magnitude of v_x deceases monotonically with N, due to finite size effect. v_x for infinite system could thus be predicted by extrapolating the asymptotic v_x–N curve. Since the computational efficiency decreases significantly with the increase of N, in this work a box containing $N = 4836$ particles is chosen. Since the box size in three dimensions are proportionally scaled, we also check the scaling effect on a $\lg v_x - \lg N$ plot in Fig. 2(b). The correlation coefficient is determined as $\zeta = 0.228$ for slip, and $\zeta = 0.225$ for non-slip boundaries.

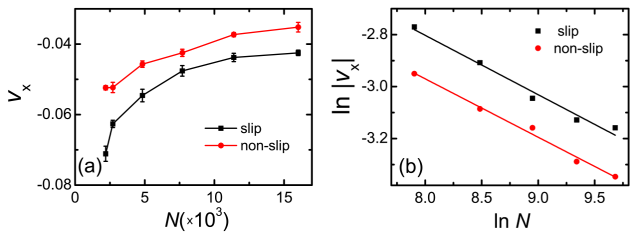

Fig. 2 The dependence of fluid velocity v_x on the number of particles N for system with slip (black) and non-slip (red) boundaries, plotted on linear (a) and double logarithmic scale (b).

2 The effect of ε_B on bound particles

We define $N_b(t)$ as the number of particles that are always bound by the colloid (i.e. $r_{ic} < r_{cut}$) within t time-steps. Fig. 3 presents the decrease of $\ln(N_b(t)/N_b(0))$ with t at different ε_B for slip

[a] Institute of Mechanics, Chinese Academy of Sciences, Beijing 100190, China
[b] Department of Chemistry, University of Cambridge, CB21EW Cambridge, UK
[c] Institute of Physics, Chinese Academy of Sciences, Beijing 100190, China
[d] Songshan Lake Materials Laboratory, Dongguan 523808, China
* jd489@cam.ac.uk
† df246@cam.ac.uk

boundaries. It shows that N_b is always larger at larger ε_B at the same t. For both (a-b) concentrated ($\rho_\beta = 0.32, |\nabla\rho_\beta| = 0.04$) and (c-d) dilute ($\rho_\beta = 0.05, |\nabla\rho_\beta| = 0.0063$) system, the density gradient (by applying 'color forces') exerts very limited effect on the decay rate of $\ln(N_b(t)/N_b(0))$. For $\varepsilon_B \geqslant 4.0$, N_b is always larger for dilute system at the same t. As $\ln(N_b(t)/N_b(0))$ decreases linearly with t, the characteristic time t_d for fluid particle bound by the colloid can be measured by fitting the slope.

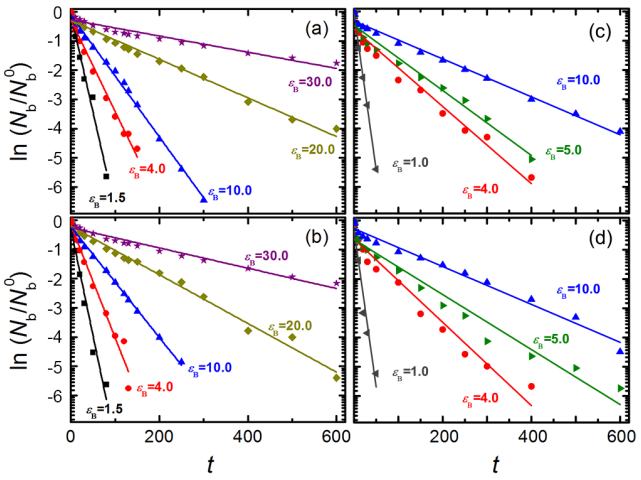

Fig. 3 $\ln(N_b(t)/N_b(0))$ versus time t at (a-b) $\rho_\beta = 0.32, |\nabla\rho_\beta| = 0.04$ and (c-d) $\rho_\beta = 0.05, |\nabla\rho_\beta| = 0.0063$ with slip boundaries. While (a) and (c) are for equilibrium system without gradient, (b) and (d) are for non-equilibrium system applying 'color' forces.

To analyze the dynamics of fluid particles surrounding the colloid, in Fig. 4 we compare typical 2D trajectories in $x-z$ plane for permanently and temporarily bound particles within 2×10^5 simulation steps at $\varepsilon_B = 10.0$. Interestingly, while permanently bound particles are localized at around $z = 0$ (i.e. $\theta = 0$ or $\theta = \pi$), we find partly bound particles are more likely to escape near $x = 0$ (i.e. $\theta = \pi/2$).

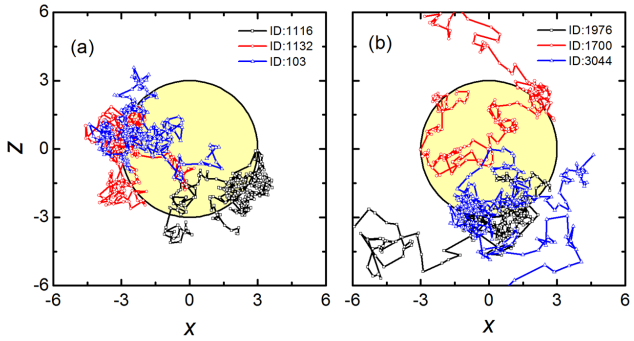

Fig. 4 2D trajectories in $x-z$ plane for (a) permanently and (b) temporarily bound particles at $\varepsilon_B = 10.0$.

To demonstrate the increase of effective size with the strength of colloid-solute interaction ε_B, we define a fictitious sphere of radius r_f, within which all solute and solvent particles are frozen (i.e. immobilized). In Fig. 5(a) below we calculate the dependence of fluid velocity v_x on r_f. At $\varepsilon_B = 1.5$ the magnitude of v_x for system with $r_f = 3.0$ is obviously smaller than that obtained for system with $r_f = 0.0$ (i.e. system without fixed fluid particles, represented by the black dashed line). However, at $\varepsilon_B = 4.0$, we find v_x is almost equal to that obtained for system with $r_f = 0.0$. This indicates that the first few layers of fluid particles (mainly solutes) are tightly bound to the colloid at strong colloid-solute interaction so that the effective size of the colloid is increased. At both $\varepsilon_B = 1.5$ and $\varepsilon_B = 4.0$, the magnitude of v_x decreases significantly with r_f, which indicates that fluids close to the colloid play an important role in generating the phoresis. When $r_f > 3.4$, as expected, the magnitude of v_x for $\varepsilon_B = 4.0$ becomes larger than that for $\varepsilon_B = 1.5$.

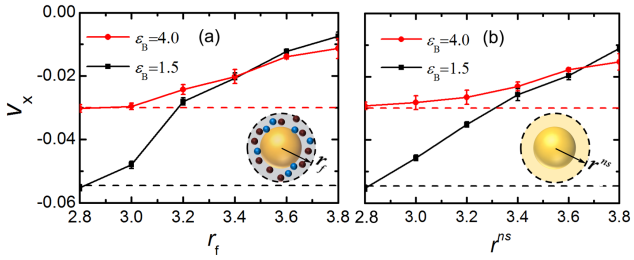

Fig. 5 The dependence of fluid velocity v_x on (a) frozen radius r_f and (b) nonslip radius r^{ns} at $\varepsilon_B = 4.0$ (red) and $\varepsilon_B = 1.5$ (black). The dashed lines indicate v_x for system with slip boundaries (i.e. $r^{ns} = 0$).

For system with non-slip boundaries, similar results are obtained for $v_x - r^{ns}$ relation shown in Fig. 5(b), where r^{ns} is the radius of non-slip boundary. At $\varepsilon_B = 1.5$ the magnitude of v_x decreases almost linearly with r^{ns}, which is much faster than that for $\varepsilon_B = 4.0$. This also indicates that the first few layers of fluid particles contribute less to phoresis at strong attraction.

To conclude, for concentrated system with large gradient ($|\nabla\rho_\beta| = 0.04$), the solute particles surrounding the colloid are not necessarily permanently bound in a shell due to solute-solute depletion and gradient force, but at large ε_B the formation of the symmetric solute shell do not contribute to phoretic flow. In addition, the magnitude of v_x surrounding the colloid is not homogeneous, thus solute particles are more likely to be bound near $\theta = 0$ or $\theta = \pi$.

3 Comparison with explicit gradient

We performed simulations with an explicit concentration gradient generated by a source and a sink region with fixed solute densities in a $36.17\times16.44\times h$ box. Comparison with the implicit gradient (color forces) results in Fig. 6 shows a aubstantially different dependence of the phoretic velocity v_x on the interaction strength ε_B. We argue that this is partly due to the finite size effects and partly due to the inherent problems within the explicit gradient simulations when the concentration and the concentration gradient of solute particles are too large.

To illustrate this claim, we analyzed the density profile of solutes from the explicit gradient simulations. In Fig. 7(a), we show the density $\rho_\beta(x)$ along the direction of concentration gradient x. We plot the densities averaged in bulk, i.e. far enough from the

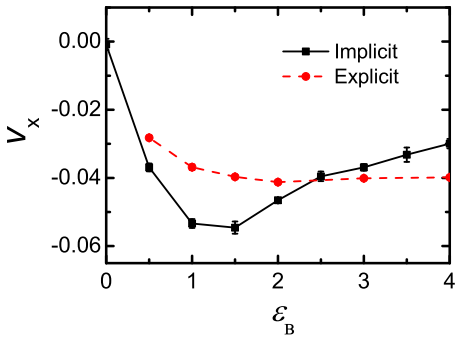

Fig. 6 Fluid velocity v_x versus solute-colloid (isotropic) interaction strength ε_B for implicit and explicit gradients, in system with $\rho_\beta = 0.32, |\nabla\rho_\beta| = 0.04$.

colloidal particle, $r_{\beta c} > 6.5$. We choose a moderate magnitude of the attraction between the solutes and the colloid ($\varepsilon_B = 2.0$), yet, for concentrated system at large gradient (black symbols, $\rho_\beta = 0.32$ and $|\nabla\rho_\beta| = 0.04$), the presence of the colloid significantly alters the profile even far away from the shaded area indicating the interaction range. Sufficiently far away from the colloid, we expect two contributions to the flux in the direction of the gradient J_β of species β: the purely diffusive term $j_d = -D\nabla\rho_\beta$, and the convective term $j_c = v_x\rho_\beta$, where v_x is the phoretic velocity (in the absence of the colloid, this term vanishes). As the total current has no source and sink, $\nabla J_\beta = \nabla(j_d + j_c) = 0$. If D and v_x are constant, this leads to an exponential profile of the solute density:

$$\rho_\beta(x) = \rho_\beta^{source} - l\nabla\rho_\beta(x_0)\, e^{-(x-x_0)/l}\,. \tag{1}$$

with the decay length $l \equiv D/\|v_x\|$ (amounting to $l = 2.88$ for $|\nabla\rho_\beta| = 0.04$ and $l' = 9.83$ for $|\nabla\rho_\beta| = 0.0063$). In Fig. 7(b), we plot the semi-log plot of the solute density from the explicit gradient simulations. The decay lengths l' fitted from this data (data for $x > 0$ are not included due to larger error) are $l' = 2.79$ for $|\nabla\rho_\beta| = 0.04$, and $l' = 6.76$ for $|\nabla\rho_\beta| = 0.0063$. The fitted l' are a bit smaller than the theoretical prediction, which might be due to finite size effect. The nonlinear effect indicates that explicit gradient method cannot be accurate especially at large Péclet number. This also explains why Sharifi-Mood et. al.[1] imposes a stepped concentration profile instead for simulations of explicit gradient.

In a dilute system with $\rho_\beta = 0.05$ and $|\nabla\rho_\beta| = 0.0063$, as shown in Fig. 8(a), we still find for $\varepsilon_B < 2.0$ the magnitude of v_x obtained from explicit gradient is smaller due to size effect, and slightly larger for $\varepsilon_B > 3.0$. However, the results obtained from explicit and implicit gradient agree well for system at even smaller gradient $|\nabla\rho_\beta| = 0.002$, shown in Fig. 8(b).

We define the scaled difference in phoretic velocity derived from explicit and implicit gradient, δv_x, as:

$$\delta v_x = \frac{v_x^{exp} - v_x^{imp}}{|v_x^{exp}|}, \tag{2}$$

where v_x^{exp} and v_x^{imp} respectively represent velocity derived from explicit and implicit gradient. Fig. 9(a) presents δv_x for two

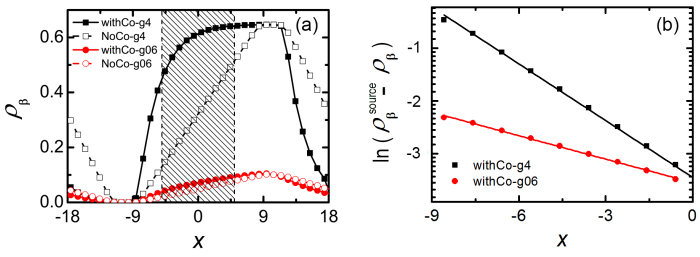

Fig. 7 Profile of (a) solute density in bulk $\rho_\beta(x)$ and (b) $\ln(\rho_\beta^{source} - \rho_\beta)$, in the direction of concentration gradient for concentrated ($\rho_\beta = 0.32$ and $|\nabla\rho_\beta| = 0.04$, black) and dilute ($\rho_\beta = 0.05$ and $|\nabla\rho_\beta| = 0.0063$, red) system at $\varepsilon_B = 2.0$. Dashed curves with hollow points are the corresponding profiles in the absence of the colloid. Shaded area represents the colloid-solute interaction range.

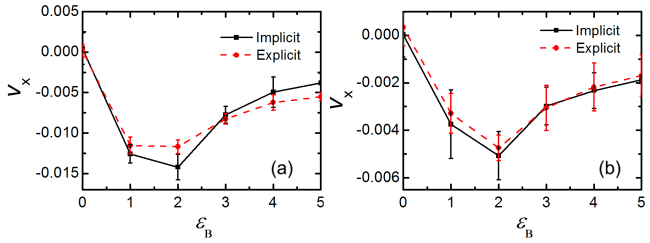

Fig. 8 Fluid velocity v_x versus solute-colloid (isotropic) interaction strength ε_B for implicit and explicit gradients, in $\rho_\beta = 0.05$ dilute system with gradient (a) $|\nabla\rho_\beta| = 0.0063$ and (b) $|\nabla\rho_\beta| = 0.002$.

different gradients, which indicates the difference is smaller for smaller gradient, especially for $\varepsilon_B > 3.0$.

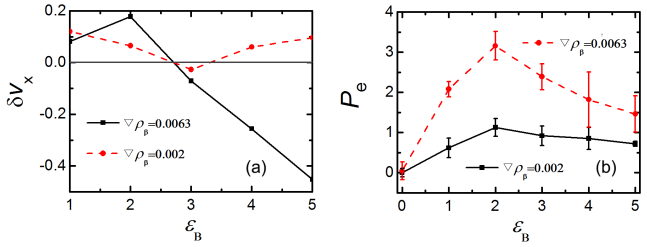

Fig. 9 (a) the dependence of scaled difference in velocity δv_x and (b) Péclet number of fluids P_e on solute-colloid (isotropic) interaction strength ε_B at different gradient.

In Fig. 9(b) we estimate the Péclet number of fluids P_e as:

$$P_e = \frac{\sigma_c v_x}{D_c}, \tag{3}$$

with D_c the diffusion coefficient of colloid determined from mean-squared displacement, v_x the phoretic flow rate and σ_c the diameter of the colloid. For any given ε_B, P_e is larger for larger $|\nabla\rho_\beta|$. The peak value of P_e is obtained at $\varepsilon_B = 2.0$ at which the magnitude of v_x reaches its maximum. For $\varepsilon_B > 2.0$, the convection term decreases faster than the diffusion term.

4 Determination of hydrodynamic radius

The generalised DA theory assumes a hard colloidal particle with non-slip boundary conditions and no flow within the colloidal hydrodynamic radius R_h (i.e. neglecting any contribution of the excess density for $r < R_h$). The theoretical prediction for the phoretic velocity is obtained by integrating the (excess) concentrations from R_h to infinity (Eq. 7 in the main text). We note that due to the attractive interactions the solute particles accumulate around the colloid and create a more or less immobile layer around it. In order to apply the theory to our model system, the original colloids (either with slip or non-slip boundaries) with diameter σ_c are replaced with effective colloids of radius R_h with non-slip boundary conditions. The magnitude of R_h is determined from analysing the mean squared displacements (MSD) of the colloid and applying the Stokes-Einstein relation. The MSD curves as a function of the interaction strength ε_B are presented in Fig. 10a) for colloids with (originally) slip boundary conditions. We see that the colloidal diffusion constant increases monotonically with ε_B. The Stokes-Einstein relation that relates R_h to the diffusion constant differs for the case of slip and non-slip boundaries. Since we know from the simulations that the DA assumption of no flow inside R_h is not entirely correct, we can assume that the real R_h is between both limits. However, already the lower limit obtained with the expression for non-slip boundaries leads to a sharp increase in R_h as a function of ε_B (see Fig. 10b). For $\varepsilon_B > 3.0$ we thus have $R_h \gtrapprox 6$ and since both the excess density of solute and solvent are close to zero for $R_h \gtrapprox 6$, the generalised DA prediction for the diffusio-phoretic velocity at strong attraction quickly approaches zero.

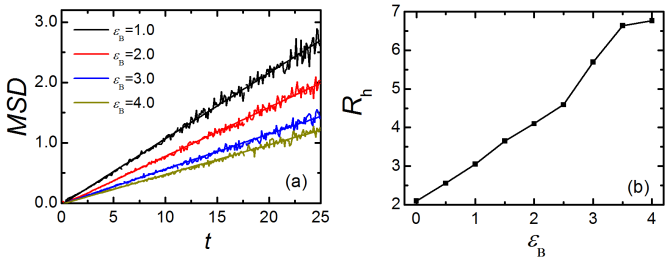

Fig. 10 (a) Mean-squared displacement of the colloid MSD(t) at solute-colloid interaction strengths between $1.0 \leqslant \varepsilon_B \leqslant 4.0$. (b) the dependence of hydrodynamic radius R_h on ε_B, as derived from the Stokes-Einstein relation by assuming non-slip boundary conditions.

5 Distribution of excess solutes

The simulation snapshots for system with anisotropic solute-colloid interaction of $l = 1$ and $l = 2$ are presented in Fig. 11. There is a polar corona of the aligned solutes surrounding the particle for $l = 1$, and symmetric distribution of solutes is observed for system of $l = 2$.

To quantitatively analyze the density distribution of solutes close to the colloid, in Fig. 12 we compare the density distributions of reduced excess solutes for different solute-colloid interactions on the $r-\theta$ plane, with r the radial distance to the colloid

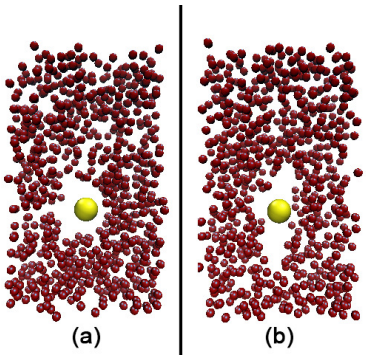

Fig. 11 Simulation snapshots for system with solute-colloid interaction in terms of (a) $P_1(\cos\theta)$ symmetry at $\lambda_B = 2.0$ and (b) $P_2(\cos\theta)$ symmetry at $\lambda_B = 2.0$. For clarity only colloid and solute particles within $-2 < y < 2$ region are shown.

and θ the opening angle over z axis (shown in Fig.1 of the main article). For $l = 2$, the distribution is almost symmetric for both positive and negative λ_B For $l = 1$, an excess of solutes is found for $\theta < \pi/4$ while a lack of solutes is found for $\theta > 3\pi/4$. These two effects cancel out so that the phoretic velocity becomes very small (the angular density distribution is almost uniform of for solvent particles). Although homogeneous density of solutes is observed for $r > r_{cut}$ for both $l = 1$ and $l = 2$, for system with isotropic interactions (i.e. $l = 0$), an excess of solutes is observed for $\theta > 3\pi/4$ and $r > r_{cut}$, as illustrated in Fig. 12(d).This explains why the magnitude of phoretic velocity depends on the system size for system with isotropic interactions, but not for system with anisotropic interactions.

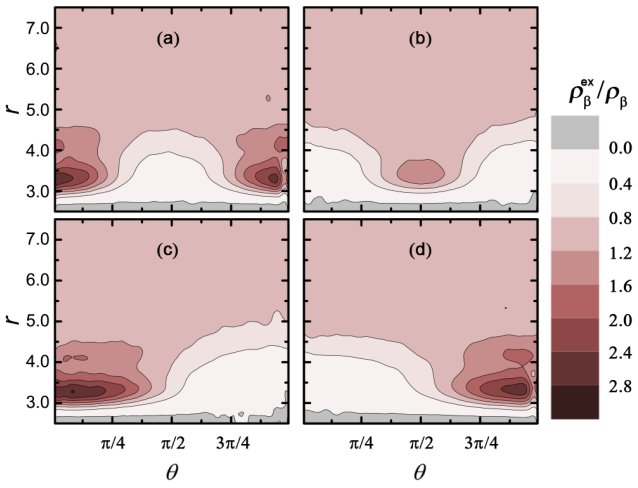

Fig. 12 The heat map plots of the fluid density in the $r-\theta$ plane for anisotropic solute-colloid interaction with symmetry $P_2(\cos\theta)$ (a,b) and $P_1(\cos\theta)$ (c,d). The interaction strength is $\lambda_B = 2.0$ (a,c) and $\lambda_B = -2.0$ (b,d).

Notes and references

1 N. Sharifi-Mood, J. Koplik and C. Maldarelli, *Phys Rev Lett*, 2013, **111**, 184501.